

Computing the gluon Sivers function at small- x

Xiaojun Yao,¹ Yoshikazu Hagiwara,² and Yoshitaka Hatta³

¹*Department of Physics, Duke University, Durham, North Carolina 27708, USA*

²*Department of Physics, Kyoto University, Sakyo-ku, Kyoto 606-8502, Japan*

³*Physics Department, Brookhaven National Laboratory, Upton, New York 11973, USA*

We compute the gluon Sivers function $f_{1T}^{\perp g}(x, k_{\perp})$ of the transversely polarized nucleon at small- x by exploiting the known connection between the dipole gluon Sivers function and the Odderon. We numerically solve the evolution equation for the Odderon both in the linear and nonlinear regimes. While we find that the x and k_{\perp} dependences of the Sivers function do not factorize as a result of the quantum evolution, factorization breaking is not numerically significant, and is much milder than what one expects in the case of unpolarized TMDs. We also point out the possibility that, due to the presence of a node in the Sivers function, single spin asymmetry for open charm production in semi-inclusive deep inelastic scattering flips signs as the transverse momentum of D-mesons is varied. This can be tested at the future Electron-Ion Collider.

I. INTRODUCTION

The Sivers function [1] is arguably the most studied transverse momentum dependent (TMD) distribution of the nucleon. It has been originally introduced by Sivers to explain large transverse single spin asymmetries (SSA) observed in polarized pp collisions $p^{\uparrow}p \rightarrow hX$. Nonvanishing parton transverse momentum k_{\perp} allows for a spin-orbit correlation of the form $k_{\perp} \times S_{\perp}$ which leads to the left-right asymmetry of parton distributions with respect to the spin vector S_{\perp} . It has now become a standard picture that SSA predominantly arises from such nonperturbative initial or final state effects. Moreover, what makes the Sivers function particularly interesting in phenomenological applications is its T-oddness. The sign change of the Sivers function between semi-inclusive DIS and Drell-Yan processes [2] is an archetypal example of the process dependence of TMD factorizations, and has been a subject of intense theoretical and experimental investigations (see [3, 4] and references therein).

While most of the literature deals with the quark Sivers function $f_{1T}^{\perp q}(x, k_{\perp})$, there is a growing interest in the gluon Sivers function $f_{1T}^{\perp g}(x, k_{\perp})$ and its possible manifestation at RHIC and the future Electron-Ion Collider (EIC) and AFTER@LHC [5–18] (see also a review [19]). On general grounds, one expects that the gluon Sivers function is an important or even dominant source of SSA for the production of high mass states such as D -mesons, J/ψ 's or dijets. It may also contribute to the SSA of light hadrons at negative x_F (Feynman variable) which is sensitive to the small- x region of the transversely polarized nucleon. However, there has been very little guidance so far, if any, from theory perspectives what should be the functional dependence of $f_{1T}^{\perp q,g}$ on x and k_{\perp} . Often the k_{\perp} -dependence is assumed to be Gaussian and factorized from the x -dependent part $f_{1T}^{\perp}(x, k_{\perp}) \sim f(x)e^{-ck_{\perp}^2}$ in phenomenological fits. However, apart from convenience, there does not seem to be a good, model-independent argument to justify such assumptions. For unpolarized TMDs, factorization is certainly broken in the small- x region where the BFKL and saturation effects are important. In particular, in the saturation regime it will be maximally violated, as TMDs depend on x and k_{\perp} through the ratio $k_{\perp}/Q_s(x)$ with $Q_s(x) \sim 1/x^{\alpha}$ being the saturation momentum. Yet, for polarized TMDs such as the Sivers function, the situation is unclear due to the lack of first principle approaches.

Recently, however, an interesting connection between the gluon Sivers function and the so-called Odderon exchange has been elucidated [7, 9, 20]. This paves the way for a numerical evaluation of the gluon Sivers function. Since the Odderon evolves leading logarithmically at small- x and the corresponding Regge intercept is exactly unity [21], one can expect that the gluon Sivers function survives at small- x . In this paper we test this possibility by solving the small- x evolution equation for the Odderon both in the linear and nonlinear regimes. We then discuss the properties of the solution and their implications in phenomenology, with particular emphasis on the factorization of x and k_{\perp} dependences.

The paper is organized as follows. In Section II, we review the relation between the gluon Sivers function and the Odderon. Then in Section III, we solve the small- x evolution equation of the Odderon, and using

this solution we compute the gluon Sivers function. Phenomenological implications of our results on the SSA in open charm production are discussed in Section IV. Section V is devoted to conclusions.

II. GLUON SIVERS FUNCTION AND ODDERON

The gluon sivers function of the nucleon f_{1T}^\perp is defined by the matrix element

$$\begin{aligned} \frac{1}{xP^+} \int \frac{dz^- d^2 z_\perp}{(2\pi)^3} e^{-ixP^+z^- + ik_\perp \cdot z_\perp} \langle PS_\perp | 2\text{Tr}[F^{+i}(z^-, z_\perp)U^{[\pm]}F^{+i}(0)U^{[\pm]}] | PS_\perp \rangle \\ = f_1^{[\pm\pm]}(x, k_\perp^2) - \frac{k_\perp \times S_\perp}{M} f_{1T}^{\perp[\pm\pm]}(x, k_\perp^2), \end{aligned} \quad (1)$$

where M is the nucleon mass and $k_\perp \times S_\perp \equiv \epsilon^{ij} k_\perp^i S_\perp^j$ with $|S_\perp| = 1$. $f_1(x, k_\perp^2)$ is the unpolarized gluon TMD normalized such that $\int d^2 k_\perp f_1(x, k_\perp^2) = G(x)$ is the usual collinear gluon PDF.¹ The trace is in the fundamental representation (e.g., $F^{+i} = F_a^{+i} t^a$) with the normalization $\text{Tr}(t^a t^b) = \frac{\delta^{ab}}{2}$.

$U^{[\pm]}$ is the lightlike, staple-shaped Wilson line connecting the points $[z, 0]$ via light-cone infinity $x^- = \pm\infty$. The choice $[++]$ or $[--]$ corresponds to the Weiszäcker-Williams (WW) Sivers function which has the property $f_{1T}^{\perp[++]} = -f_{1T}^{\perp[--]}$ due to PT symmetry. This is the gluonic counterpart of the sign change of the quark Sivers function, and can be tested experimentally [10, 13]. On the other hand, the choice $[+-]$ or $[-+]$ gives the dipole Sivers function. Again, from PT symmetry it follows that $f_{1T}^{\perp[+-]} = -f_{1T}^{\perp[-+]}$.

We shall be interested in the small- x behavior of f_{1T}^\perp . As observed in [9], the WW Sivers function is suppressed at small- x . On the other hand, the dipole Sivers function develops leading logarithms $\alpha_s \ln 1/x$ and therefore it has a chance to survive in the small- x region. Indeed, neglecting x in the exponential factor of (1), we can approximate the left hand side as, for the component $[+-]$,

$$\frac{4N_c k_\perp^2}{xg^2} \int \frac{d^2 x_\perp d^2 y_\perp}{(2\pi)^3} e^{ik_\perp \cdot (x_\perp - y_\perp)} S(x_\perp, y_\perp), \quad (2)$$

where S is the so-called dipole S-matrix

$$S(x_\perp, y_\perp) = \frac{\langle PS | \frac{1}{N_c} \text{Tr} U^\dagger(x_\perp) U(y_\perp) | PS \rangle}{\langle PS | PS \rangle}, \quad (3)$$

with

$$U(y_\perp) = P \exp \left(-ig \int_{-\infty}^{\infty} dz^- A^+(z^-, y_\perp) \right). \quad (4)$$

The second term of (1) is odd in k_\perp , so the Sivers function is related to the imaginary part of the S-matrix which is odd in $x_\perp - y_\perp = r_\perp$. To see this more explicitly, we parameterize as

$$S(x_\perp, y_\perp) = P(|r_\perp|) + iS_\perp \times r_\perp Q(|r_\perp|), \quad (5)$$

where P, Q are real. P is commonly referred to as the Pomeron, whereas the imaginary part of the dipole S-matrix has been identified with the Odderon [23]. Since the Odderon amplitude is a scalar function and odd in r_\perp , it vanishes unless there is a reference vector other than r_\perp . For the transversely polarized nucleon, the transverse spin S_\perp provides such a vector.² The resulting Odderon term has the structure (5) and has been dubbed the spin-dependent Odderon [7, 20].

Now consider the Fourier transform of (5)

$$\int d^2 r_\perp S(x_\perp, y_\perp) e^{ik_\perp \cdot r_\perp} = \tilde{P}(|k_\perp|) + S_\perp \times k_\perp \tilde{Q}(|k_\perp|), \quad (6)$$

¹ Our normalization of f_1 and f_{1T}^\perp differs from that of [9] by a factor of 2, see (2) of [9] and sum over the indices $\mu\nu$.

² Another example is that if one considers the nonforward amplitude $\langle P' | \text{Tr} U_x^\dagger U_y | P \rangle$, the momentum transfer $\Delta_\perp = P'_\perp - P_\perp$ provides a reference vector. This is equivalent to consider the dipole S-matrix as a function also of the impact parameter $b_\perp = \frac{x_\perp + y_\perp}{2}$. The Odderon term has the structure $b_\perp \cdot r_\perp$ in this case [26].

where

$$\tilde{Q}(|k_\perp|) = \frac{i}{k_\perp^2} \int d^2 r_\perp e^{ik_\perp \cdot r_\perp} k_\perp \cdot r_\perp Q(|r_\perp|) = -\frac{2\pi}{|k_\perp|} \int_0^\infty d|r_\perp| r_\perp^2 J_1(|k_\perp| |r_\perp|) Q(|r_\perp|), \quad (7)$$

is now a real function. Substituting this into (2), one gets [7, 9]

$$\frac{N_c k_\perp^2 M}{2g^2 \pi^3} \mathcal{A} \tilde{Q}(|k_\perp|) = x f_{1T}^\perp(x, k_\perp^2), \quad (8)$$

where \mathcal{A} is the transverse area of the nucleon and the superscript $[+-]$ has been omitted. In the literature, often the notation $\Delta^N f$ is used instead of f_{1T}^\perp . Their relation is (see (2) of [8])

$$\Delta^N f(|k_\perp|) = -2 \frac{|k_\perp|}{M} f_{1T}^\perp(|k_\perp|) = -\frac{|k_\perp|^3 N_c}{4\pi^4 \alpha_s x} \mathcal{A} \tilde{Q}(|k_\perp|). \quad (9)$$

III. NUMERICAL SOLUTION OF THE ODDERON EQUATION

A. Evolution equation

So far we have kept the x -dependence of the Pomeron and Odderon amplitudes implicit. The dependence comes from the small- x evolution which we now turn to. The dipole S-matrix satisfies the Balitsky-Kovchegov equation

$$\frac{\partial}{\partial Y} S(x_\perp, y_\perp) = \frac{\bar{\alpha}_s}{2\pi} \int \frac{d^2 z_\perp}{(2\pi)^2} \frac{(x_\perp - y_\perp)^2}{(x_\perp - z_\perp)^2 (z_\perp - y_\perp)^2} (S(x_\perp, z_\perp) S(z_\perp, y_\perp) - S(x_\perp, y_\perp)), \quad (10)$$

where $\bar{\alpha}_s \equiv \frac{\alpha_s N_c}{\pi}$ and $Y = \ln \frac{x_0}{x}$ is the rapidity. (x_0 is some starting value.) By decomposing (10) into the real and imaginary parts using (5), one obtains the small- x evolution equations for the Pomeron and Odderon. Let us denote

$$P(x_\perp, y_\perp) = 1 - N(x_\perp, y_\perp), \quad S_\perp \times r_\perp Q(x_\perp, y_\perp) = O(x_\perp, y_\perp). \quad (11)$$

Then the equations read [22, 23]

$$\begin{aligned} \frac{\partial}{\partial Y} O(x_\perp, y_\perp) = \frac{\bar{\alpha}_s}{2\pi} \int d^2 z_\perp \frac{(x_\perp - y_\perp)^2}{(x_\perp - z_\perp)^2 (z_\perp - y_\perp)^2} & \left[O(x_\perp, z_\perp) + O(z_\perp, y_\perp) - O(x_\perp, y_\perp) \right. \\ & \left. - O(x_\perp, z_\perp) N(z_\perp, y_\perp) - N(x_\perp, z_\perp) O(z_\perp, y_\perp) \right], \end{aligned} \quad (12)$$

$$\begin{aligned} \frac{\partial}{\partial Y} N(x_\perp, y_\perp) = \frac{\bar{\alpha}_s}{2\pi} \int d^2 z_\perp \frac{(x_\perp - y_\perp)^2}{(x_\perp - z_\perp)^2 (z_\perp - y_\perp)^2} & \left[N(x_\perp, z_\perp) + N(z_\perp, y_\perp) - N(x_\perp, y_\perp) \right. \\ & \left. - N(x_\perp, z_\perp) N(z_\perp, y_\perp) + O(x_\perp, z_\perp) O(z_\perp, y_\perp) \right]. \end{aligned} \quad (13)$$

Let θ be the azimuthal angle in the transverse plane measured with respect to S_\perp . Then $O \propto \sin \theta$ and the last term $\sim OO$ in (13) induces an angular dependence $\sim \cos 2\theta$ in N even if it is initially independent of θ .³ This in turn induces a $\sin \theta \cos 2\theta$ dependence in O via (12) (or $\cos 2\theta$ dependence in Q). By repeating this argument, N and Q eventually depend on arbitrary even harmonics $\cos 2n\theta$.

The equation for the Odderon has been previously solved numerically in [24], but the connection to spin physics was not explored. We shall present our numerical solution of the coupled equation (12) and (13), and study the dependence of the gluon Sivers function on x and k_\perp .

³ It should be noted that Ref. [22] dismissed this term as a higher order effect which should not be kept consistently to the order of accuracy (i.e., leading logarithmic approximation). However, we keep this term as it brings in qualitatively new interesting features. In any case, the effect of this term is numerically very small.

B. Setup

Since the Sivers function is a forward matrix element we can assume translational invariance and neglect the dependence of N and O on the impact parameter $b_\perp = \frac{x_\perp + y_\perp}{2}$. We can then set y_\perp as the origin and switch to the polar coordinates so that $S(x_\perp, y_\perp) = S(x_\perp - y_\perp) = S(r_\perp) = S(|r_\perp|, \theta)$. Without loss of generality, we choose the spin vector S_\perp to be along the positive x -axis, so θ is measured with respect to this axis.

The initial conditions are [7]

$$N(|r_\perp|, \theta) = 1 - e^{-r_\perp^2 Q_{s0}^2}, \quad O(|r_\perp|, \theta) = \kappa Q_{s0}^3 |r_\perp|^3 \sin \theta e^{-r_\perp^2 Q_{s0}^2}, \quad (14)$$

at $Y = 0$, where Q_{s0} is the initial saturation scale. In principle, the constant κ can be determined along the line of [7, 25],⁴ but here we consider it as an unknown, including its sign. The following numerical results are obtained for $\kappa = \frac{1}{3}$. Since the evolution equation is essentially linear in O (the nonlinear term OO in (13) is numerically tiny), the normalization and the sign can be adjusted later. It can be also fitted by comparing with the future experimental data at the EIC.

To calculate the integral over z_\perp , we discretize it by setting up a lattice in $|r_\perp|$ and θ . We rescale $|r_\perp|$ by Q_{s0} so the calculation is carried out in a unitless way with $|\tilde{r}_\perp| \equiv |r_\perp| Q_{s0}$. The lattice on $|\tilde{r}_\perp|$ is uniform in $\ln |\tilde{r}_\perp|$ from $\ln |\tilde{r}_\perp| = -12$ to 4 with the number of lattice sites $n_{|r_\perp|} = 400$. The lattice on θ is uniform from 0 to 2π with the number of sites $n_\theta = 100$. We set $\bar{\alpha}_s = \frac{\alpha_s N_c}{\pi} = 0.2$ throughout the paper. We solve the evolution in Y by discretizing $\Delta Y = 0.4$ and use the Runge-Kutta 4th order method. At each evolution step ΔY , we update the value of N and O at each lattice site. The points of $x_\perp - y_\perp$ and $z_\perp - y_\perp$ are on the lattice, but the points of $x_\perp - z_\perp$ are not in general. So to obtain the values of N and O at the points $x_\perp - z_\perp$, a linear interpretation among the lattice sites is applied.

C. Results

We plot the values of N and O at different Y 's along the axis of $\theta = \pi/2$ in Fig. 1. The Pomeron amplitude N shows the familiar ‘geometric scaling’ with the inflection point inversely related to the saturation scale $Q_s(Y) \propto e^{\#Y}$. The peak location of the Odderon also moves with Y , but its dependence is significantly weaker. This is presumably related to the observation in [27] that any angular dependence of the dipole S-matrix comes with extra powers of r_\perp , and this kills the geometric scaling structure. On the other hand, the magnitude of the Odderon amplitude rapidly decreases with Y . This is due to the nonlinear terms in (12). Indeed, if $N \approx 1$ in the saturation regime, only the virtual term $-O(x_\perp, y_\perp)$ survives on the right hand side of (12), and this leads to a strong Sudakov suppression of O . To elaborate on this point, in Fig. 2 we show our numerical solution without the nonlinear terms $\sim NO + ON$ (starting from the same initial condition).⁵ From the ‘BLV’ Odderon solution [21], one expects that the amplitude is constant in Y . However, this is so only in a very limited sense. We see indeed that the magnitude of O around $|r_\perp| \sim 2Q_{s0}^{-1}$ is almost independent of Y , but the smaller- or larger- r_\perp regions strongly depend on Y . In the small- r_\perp region the first two terms in (12) nearly cancel $O(r_\perp - z_\perp) + O(z_\perp) \approx O(-z_\perp) + O(z_\perp) = 0$, and therefore the amplitude receives an exponential Sudakov suppression in Y . In the large- r_\perp region, the first and third terms cancel and we are left with the second term $O(z_\perp)$ which is positive. Therefore, the amplitude in the large- r_\perp region tends to increase and becomes sensitive to the finite volume effects as well as the nonperturbative effects. In this regard it is interesting to see that the nonlinear terms cut off this sensitivity and make the large- r_\perp behavior drastically different.

Turning to the θ -dependence, in Fig. 3 we fix $Y = 4$ and $|r_\perp|$ and plot N as a function of θ . We notice that during the evolution in Y , the Pomeron N gains a $\cos 2\theta$ dependence. This comes from the OO term in the evolution equation as discussed in Section. III A. However, the dependence is extremely weak—the oscillation magnitude in θ is of order 5×10^{-5} . This tiny number is approximately given by $\frac{\bar{\alpha}_s}{2\pi} Y O^2$ if we

⁴ There is also a constraint on the value of κ from group theory [24].

⁵ Since we noticed that in this case the large- r_\perp region is not suppressed, we solved the equation on a square lattice (x, y) (not in $\ln \tilde{r}_\perp$) with each side from -8 to 8 (scaled by Q_{s0}^{-1}) and having 300 lattice sites.

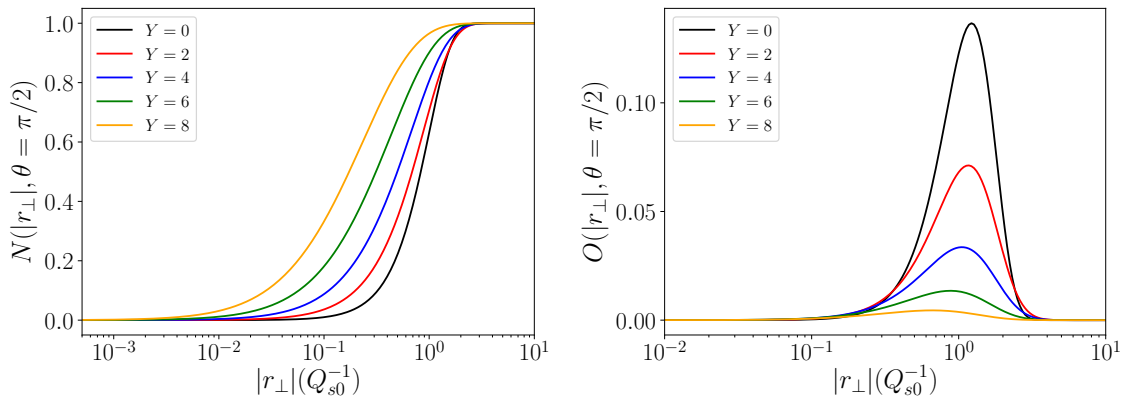


FIG. 1. N and O as functions of $|r_\perp|$ along the axis of $\theta = \pi/2$.

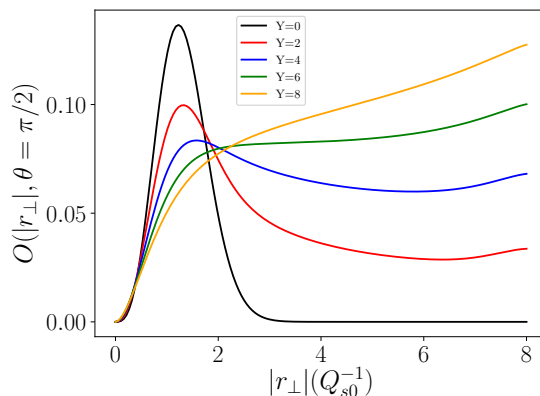


FIG. 2. Odderon solution in the linear evolution equation along the axis of $\theta = \pi/2$.

take $Y = 4$ and $O \approx 0.02$. In principle, N and O will continue influencing each other and develop higher order even harmonics. However, higher order cosine terms are numerically negligible, as can be seen in Fig. 3. The contour plot of (6) in the k_\perp plane at $Y = 4$ is shown in Fig. 4. It shows the deformation characteristic to the Siverson function.

The result of the gluon Siverson function is plotted in Fig. 5. There is a characteristic node for all values of Y which is inherited from the node in $\tilde{Q}(k_\perp)$ as pointed out in [7]. We also find that the peak region at small- k_\perp remains approximately Gaussian $\sim |k_\perp|^n e^{-k_\perp^2/\langle k_\perp^2 \rangle}$ up to large- Y , with some Y -dependence in the width $\langle k_\perp^2 \rangle$ as shown in Fig. 6. This means that the $Y = \ln 1/x$ and k_\perp dependences of the Siverson function do not factorize. The fact that the zero-crossing point in k_\perp depends on Y is also a signal of factorization breaking. However, these effects are rather mild. In the case of unpolarized TMDs, one expects a strong factorization breaking in the small- x regime since both the BFKL and saturation effects induce strong correlations between x and k_\perp . In particular, in the latter regime distributions typically depend on the ratio $k_\perp/Q_s(Y)$. However, $\langle k_\perp^2 \rangle$ has a much weaker Y -dependence than $Q_s(Y) \sim e^{\#Y}$. As we pointed out already, this is related to the fact that the Odderon is an angular dependent part of the dipole amplitude. It thus seems that factorization is not a bad approximation for the gluon Siverson function (and therefore also the sea-quark Siverson function [16]).

On the other hand, simple Gaussian parametrizations completely miss the node, and hence the sign change of the Siverson function at large- k_\perp . As we shall demonstrate shortly, this sign change has an interesting observable consequence.

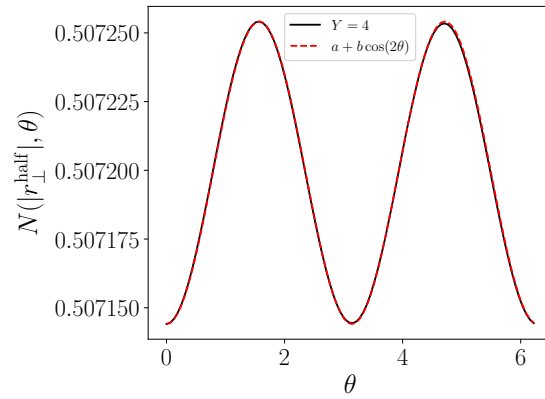


FIG. 3. N as functions of θ at fixed $|r_{\perp}|$. N is evaluated at the point $N(|r_{\perp}^{\text{half}}|) = 0.5$. The black solid curves represent the numerical solution of the evolution equation while the red dashed curves are fitted results.

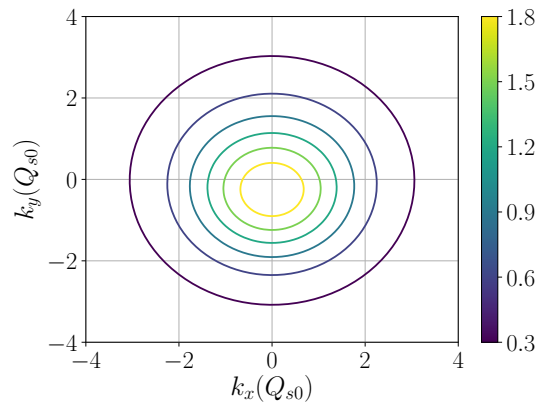


FIG. 4. Contour plot of (6) in the transverse momentum plane at $Y = 4$. The spin is pointing in the $+x$ direction.

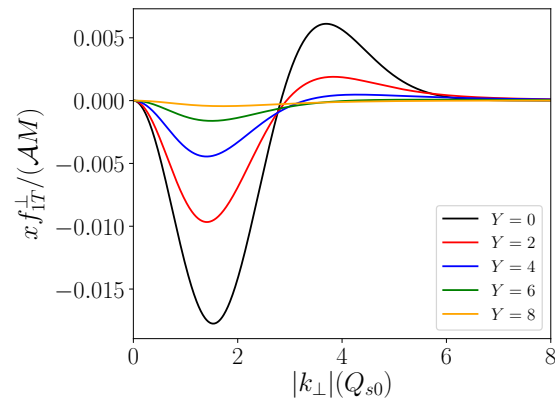


FIG. 5. $x f_{1T}^{\perp}(|k_{\perp}|)$ at different Y 's. The normalization, including the overall sign, is arbitrary as it depends on the unknown constant κ .

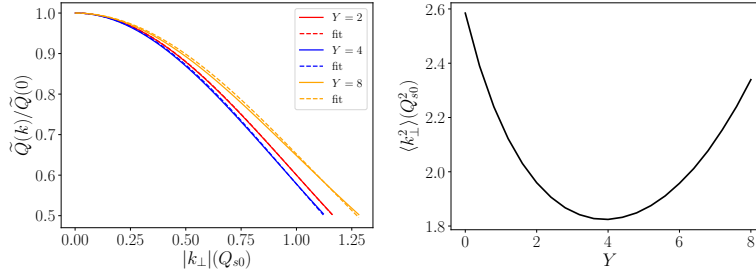


FIG. 6. Left: Gaussian fitting of $\tilde{Q}(k_\perp)/\tilde{Q}(0)$ (note that $f_{1T}^\perp(k_\perp) \sim k_\perp^2 \tilde{Q}(k_\perp)$, see (8)). Solid lines are the numerical solutions while dashed lines are the fitting results. Right: the fitted $\langle k_\perp^2 \rangle$ as a function of Y .

IV. SSA IN OPEN CHARM PRODUCTION

Finally in this section we make a connection to observables. An interesting process in which the dipole gluon Sivers function plays a role is single spin asymmetry in open charm production $ep^\uparrow \rightarrow D^0 X, \bar{D}^0 X$ in semi-inclusive DIS [7, 11, 13]. The spin-dependent part of the differential cross section of charm quark production reads

$$\frac{d\sigma}{dx_B dz dQ^2 dy d^2\ell_\perp} = \frac{\alpha_{\text{em}}^2 e_c^2}{2\pi^4 x_B Q^2} \mathcal{A} \int \frac{d^2 k_\perp}{(2\pi)^2} H(k_\perp, \ell_\perp, Q^2) \epsilon^{ij} S_{\perp i} k_{\perp j} \tilde{Q}(|k_\perp|), \quad (15)$$

where

$$\begin{aligned} H(k_\perp, \ell_\perp, Q^2) = & \left[1 - y + \frac{y^2}{2}\right] \left\{ (z^2 + (1-z)^2) \left[\frac{\ell_\perp - k_\perp}{\rho + (\ell_\perp - k_\perp)^2} - \frac{\ell_\perp}{\rho + \ell_\perp^2} \right]^2 \right. \\ & \left. + m_c^2 \left(\frac{1}{\rho + (\ell_\perp - k_\perp)^2} - \frac{1}{\rho + \ell_\perp^2} \right)^2 \right\} \\ & + 4(1-y)z^2(1-z)^2 Q^2 \left(\frac{1}{\rho + (\ell_\perp - k_\perp)^2} - \frac{1}{\rho + \ell_\perp^2} \right)^2. \end{aligned} \quad (16)$$

The first two lines are contributions from the transversely polarized virtual photon while the last line is the contribution from the longitudinally polarized one. The kinematic variables are defined as follows: $Q^2 = -q^2$, $x_B = Q^2/2P \cdot q$, $y = P \cdot q/P \cdot k$, $z = P \cdot \ell/P \cdot q$ and $\rho = z(1-z)Q^2 + m_c^2$ where m_c is the charm quark mass, and k , P , q and ℓ are the momenta of the incoming electron and proton, the transferred photon and the produced charm quark respectively. Compared to the formula in [7], we have included the charm quark mass and also added the contribution from the longitudinally polarized virtual photon (cf. [28]).

Let us consider the following integral

$$\int d^2 k_\perp H(k_\perp, \ell_\perp, Q^2) k_{\perp j} \tilde{Q}(|k_\perp|) \equiv \hat{\ell}_{\perp j} I_c(|\ell_\perp|), \quad (17)$$

where we have used the fact that after integrating over k_\perp , the integral should be proportional to $\ell_{\perp j}$. The proportionality constant depends on $|\ell_\perp|$ and can be evaluated straightforwardly using our numerical solution for $\tilde{Q}(k_\perp)$. Since $H(k_\perp)$ is suppressed when k_\perp is small, we expect that the integral is dominated around $k_\perp \sim \ell_\perp$. Then an interesting possibility arises that the node in $\tilde{Q}(k_\perp)$ is transferred to a node in the ℓ_\perp -spectrum.

We assume $m_c = 1.3$ GeV, $Q_{s0} = 0.7$ GeV and evaluate I_c for $y = z = 1/2$ and different values of Q^2 . We first plot in Fig. 7 (left) the contribution coming only from the first line of (16). As expected, we see very clearly a sign change roughly around the same value of transverse momentum where \tilde{Q} changes signs. However, the situation becomes more complicated once the other terms are included. Actually,

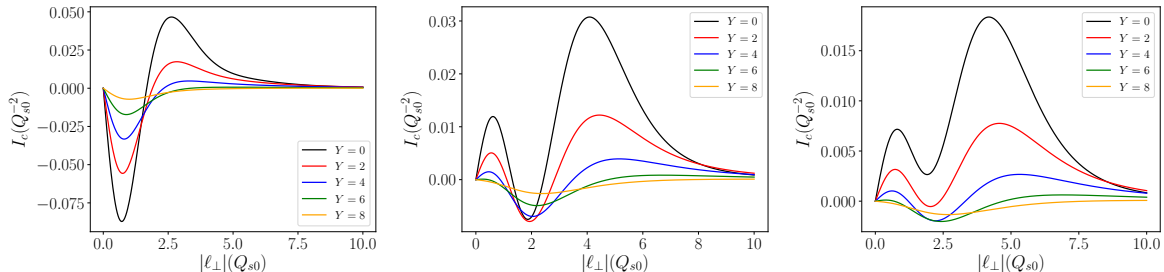


FIG. 7. Left: $I_c(|\ell_\perp|)$ from the transversely polarized virtual photon in the massless quark limit at $Q^2 = 5$ GeV. Middle: $I_c(|\ell_\perp|)$ at $Q^2 = 1$ GeV. Right: $I_c(|\ell_\perp|)$ at $Q^2 = 5$ GeV.

unless Q^2 is very large, the middle term of (16) is always dominant and this flips the sign of I_c in the low- ℓ_\perp region. As a result, the SSA flips signs twice as the transverse momentum of the produced charm quark is varied. This is shown in the middle plot of Fig. 7. The signal gradually decreases and the sign flipping almost disappears with increasing Q^2 .⁶ But the valley structure in the SSA as a function of transverse momentum still exists. It is thus very interesting to vary Q^2 in experiments and explore these different possibilities.

V. CONCLUSIONS

In this paper we have computed the (dipole) gluon Siverson function at small- x by numerically solving the evolution equation for the Odderon [22, 23]. Our results convey several important messages which should be considered when modeling the Siverson function. Firstly, the factorization breaking of the x and k_\perp -dependences of the Siverson function is rather mild, in contrast to the unpolarized TMDs which is related to the Pomeron part of the dipole amplitude. This seems to be a generic feature of the angular dependent part of the Wilson line correlators (cf. [27]), and thus we expect that the situation is similar for the Weizsäcker-Williams gluon Siverson function. In other words, assuming factorization may not be a bad approximation, although systematic deviations do exist. Secondly, the amplitude of the Siverson function decreases monotonically in Y in the large- k_\perp (small- r_\perp) region in the linear evolution regime, and everywhere in the nonlinear regime. This is due to the dominance of the virtual term $-O(x_\perp, y_\perp)$ in the evolution equations which leads to an exponential suppression. Finally, the dipole gluon Siverson function has a node [7] for all values of x . This leads to interesting observable consequences: the SSA in open charm production $ep^\uparrow \rightarrow DX$ in SIDIS changes signs, possibly twice, as a function of the D-meson transverse momentum at low- Q^2 . Note also that SSA for D^0 mesons has an opposite sign from that for \bar{D}^0 mesons due to the C-odd nature of the Odderon [7, 29, 30]. On top of this, there is the ‘usual’ sign change in the Weizsäcker-Williams gluon Siverson function that can be tested in ep^\uparrow and pp^\uparrow collisions [10]. All these make the studies of the gluon Siverson function very fascinating, and we look forward to a rich phenomenology at experimental facilities such as RHIC, AFTER@LHC and EIC.

ACKNOWLEDGMENTS

We are grateful to Jian Zhou for discussions and for reading the draft of this paper. We also thank Piet Mulders and Feng Yuan for discussion. This material is based on work supported by the U. S. Department of Energy, Office of Science, Office of Nuclear Physics under Contract No. DE-SC0012704. It is also supported in part by a LDRD grant from Brookhaven Science Associates. X.Y. thanks the nuclear

⁶ This is consistent with the TMD evolution effects which tend to diminish the node structure at high- Q^2 [16].

theory group at Brookhaven National Laboratory, where this work was completed, for its hospitality. X.Y. is supported by U.S. Department of Energy under Research Grant No. DE-FG02-05ER41367. X.Y. also acknowledges support from Brookhaven National Laboratory. Y. Hagiwara is supported by the JSPS KAKENHI Grant No. 17J08072.

-
- [1] D. W. Sivers, Phys. Rev. D **41**, 83 (1990).
 - [2] J. C. Collins, Phys. Lett. B **536**, 43 (2002) [hep-ph/0204004].
 - [3] L. Adamczyk *et al.* [STAR Collaboration], Phys. Rev. Lett. **116**, no. 13, 132301 (2016) [arXiv:1511.06003 [nucl-ex]].
 - [4] M. Aghasyan *et al.* [COMPASS Collaboration], Phys. Rev. Lett. **119**, no. 11, 112002 (2017) [arXiv:1704.00488 [hep-ex]].
 - [5] M. Anselmino, M. Boglione, U. D'Alesio, E. Leader and F. Murgia, Phys. Rev. D **70**, 074025 (2004) [hep-ph/0407100].
 - [6] F. Yuan, Phys. Rev. D **78**, 014024 (2008) [arXiv:0801.4357 [hep-ph]].
 - [7] J. Zhou, Phys. Rev. D **89**, no. 7, 074050 (2014) [arXiv:1308.5912 [hep-ph]].
 - [8] U. D'Alesio, F. Murgia and C. Pisano, JHEP **1509**, 119 (2015) [arXiv:1506.03078 [hep-ph]].
 - [9] D. Boer, M. G. Echevarria, P. Mulders and J. Zhou, Phys. Rev. Lett. **116**, no. 12, 122001 (2016) [arXiv:1511.03485 [hep-ph]].
 - [10] D. Boer, P. J. Mulders, C. Pisano and J. Zhou, JHEP **1608**, 001 (2016) [arXiv:1605.07934 [hep-ph]].
 - [11] R. M. Godbole, A. Kaushik and A. Misra, Phys. Rev. D **97**, no. 7, 076001 (2018) [arXiv:1709.03074 [hep-ph]].
 - [12] V. P. Goncalves, Phys. Rev. D **97**, no. 1, 014001 (2018) [arXiv:1710.01674 [hep-ph]].
 - [13] L. Zheng, E. C. Aschenauer, J. H. Lee, B. W. Xiao and Z. B. Yin, Phys. Rev. D **98**, no. 3, 034011 (2018) [arXiv:1805.05290 [hep-ph]].
 - [14] C. Hadjidakis *et al.*, arXiv:1807.00603 [hep-ex].
 - [15] S. Rajesh, R. Kishore and A. Mukherjee, Phys. Rev. D **98**, no. 1, 014007 (2018) [arXiv:1802.10359 [hep-ph]].
 - [16] H. Dong, D. X. Zheng and J. Zhou, arXiv:1805.09479 [hep-ph].
 - [17] R. M. Godbole, A. Kaushik, A. Misra and S. Padval, arXiv:1810.07113 [hep-ph].
 - [18] U. D'Alesio, C. Flore, F. Murgia, C. Pisano and P. Taels, arXiv:1811.02970 [hep-ph].
 - [19] D. Boer, C. Lorce, C. Pisano and J. Zhou, Adv. High Energy Phys. **2015**, 371396 (2015) [arXiv:1504.04332 [hep-ph]].
 - [20] L. Szymanowski and J. Zhou, Phys. Lett. B **760**, 249 (2016) [arXiv:1604.03207 [hep-ph]].
 - [21] J. Bartels, L. N. Lipatov and G. P. Vacca, Phys. Lett. B **477**, 178 (2000) [hep-ph/9912423].
 - [22] Y. V. Kovchegov, L. Szymanowski and S. Wallon, Phys. Lett. B **586**, 267 (2004) [hep-ph/0309281].
 - [23] Y. Hatta, E. Iancu, K. Itakura and L. McLerran, Nucl. Phys. A **760**, 172 (2005) [hep-ph/0501171].
 - [24] T. Lappi, A. Ramnath, K. Rummukainen and H. Weigert, Phys. Rev. D **94**, no. 5, 054014 (2016) [arXiv:1606.00551 [hep-ph]].
 - [25] S. Jeon and R. Venugopalan, Phys. Rev. D **71**, 125003 (2005) [hep-ph/0503219].
 - [26] Y. V. Kovchegov and M. D. Sievert, Phys. Rev. D **86**, 034028 (2012) Erratum: [Phys. Rev. D **86**, 079906 (2012)] [arXiv:1201.5890 [hep-ph]].
 - [27] Y. Hagiwara, Y. Hatta and T. Ueda, Phys. Rev. D **94**, no. 9, 094036 (2016) [arXiv:1609.05773 [hep-ph]].
 - [28] C. Marquet, B. W. Xiao and F. Yuan, Phys. Lett. B **682**, 207 (2009) [arXiv:0906.1454 [hep-ph]].
 - [29] H. Beppu, Y. Koike, K. Tanaka and S. Yoshida, Phys. Rev. D **82**, 054005 (2010) [arXiv:1007.2034 [hep-ph]].
 - [30] Z. B. Kang and J. W. Qiu, Phys. Rev. D **78**, 034005 (2008) [arXiv:0806.1970 [hep-ph]].